PERFORM
Evaluation of the H_2S removal technique

Deliverable 3.3

Prepared by: Party: GFZ and Hi,
Simona Regenspurg (GFZ)
Joy Ianotta (HI)

Checked by: Party: Florian Eichinger, Viola van Pul-Verboom

PERFORM is one of nine projects under the GEOTHERMICA – ERA NET The overarching target of PERFORM is to improve geothermal system performance, lower operational expenses and extend the life-time of infrastructure by the concept of combining data collection, predictive modelling, innovative technology development and in-situ validation. The improvement of geothermal plant performance from the proposed work is expected to result in an increase of the energy output by 10 to 50%. In order to reach this goal PERFORM will establish a single and shared knowledge database, build predictive models and demonstrate new and improved, cost-effective technologies which will reduce or even eliminate flow-obstructive scaling, clogging, and resistance to fluid (re-)injection at eight geothermal plants across Europe.

The GEOTHERMICA is supported by the European Union's HORIZON 2020 programme for research, technological development and demonstration under grant agreement No 731117

About PERFORM

Despite years of experience with geothermal systems, the geothermal sector still faces a significant number of underperforming doublets, posing a strong limitation on a region's growth of geothermal energy utilization. A key operational challenge in geothermal energy production is restricted flow. Major obstacles for geothermal flow are scaling (mineral deposition), clogging (solid micro-particle deposition), corrosion and inefficient injection strategies. These issues result in high and mostly unforeseen costs for workovers, and additionally reduce production. In order to overcome these challenges, the consolidation and sharing of knowledge, including validated strategies for prevention and mitigation needs to be in place.

Therefore a consortium consisting of De Nationale Geologiske Undersøgelser for Danmark og Grønland (GEUS) and FORCE Technology from Denmark, Helmholtz Centre Potsdam German Research Centre for Geosciences (GFZ) and Hydroisotop GmbH from Germany and Ammerlaan Geothermie B.V., Greenwell Westland B.V., Wageningen Food & Biobased Research and ECN part of TNO from the Netherlands proposed a GEOTHERMICA project PERFORM, which has been granted. The overarching target of PERFORM is to improve geothermal system performance, lower operational expenses and extend the life-time of infrastructure by the concept of combining data collection, predictive modelling, innovative technology development and in-situ validation. The improvement of geothermal plant performance from the proposed work is expected to result in an increase of the energy output by 10 to 50%. In order to reach this goal PERFORM will establish a single and shared knowledge database, build predictive models and demonstrate new and improved, cost-effective technologies which will reduce or even eliminate flow-obstructive scaling, clogging, and resistance to fluid (re-)injection at eight geothermal plants across Europe.

Based on experiences from operating geothermal sites within the EU, PERFORM will establish a single knowledge database containing information on operational, chemical and physical aspects of geothermal energy production. The database enables sharing experiences from operating geothermal doublets located in various countries and comparing the performance of the different geothermal reservoirs.
PERFORM builds predictive models that allow for pinpointing the most likely sources and causes of failure, as well as the best options for injectivity improvement. The integrated models will provide forecasting for scaling, productivity, and injectivity on short- and long- time scales, supporting early warning and planning of mitigation measures. Coupled thermo-hydro-mechanical-chemical simulators will allow for evaluation of injection temperature that apart for increasing flow will also increase the energy output.

Data and knowledge gathering and technology demonstration is planned for eight geothermal plants across Europe. Demonstration of new and improved, cost-effective technologies will allow for the reduction or even elimination of flow-obstructive scaling, clogging, and resistance to fluid (re-)injection. The technologies include low-cost cation extraction filters, self-cleaning particle removal appliances, H_2S removal technology and soft-stimulating injection procedures (thermal and CO_2-injection). The goal is to provide a set of new and improved, low-cost and environmentally friendly technology alternatives.
PERFORM integrates the knowledge database, predictive modelling and advanced technologies into a design and operation toolbox, which will be tied to economical calculations. The toolbox will enable stakeholders and specifically geothermal operators to plan future operations, mitigate existing obstructions, and optimise production/injection procedures, thus ensuring maximum energy production when needed.

This project has been subsidized through the ERANET Cofund GEOTHERMICA (Project no. 731117), from the European Commission, Topsector Energy subsidy from the Ministry of Economic Affairs of the Netherlands, Federal Ministry for Economic Affairs and Energy of Germany and EUDP.

Summary

A new method to remove hydrogen sulfide from geothermal water during operation of a production well was tested at the geothermal site (thermal bath) Oberlaa in Vienna (Austria). For this purpose Fe(III) was added either as granulated iron hydroxide or as $FeCl_3$ solution into a reaction vessel containing the thermal water that was directly removed from the wells. Physicochemical parameters as well as sulfide were measured constantly over time both, in the water from the container outlet as well as right after passing a particle filter.

It was found that the sulfide could be fully removed from the water by both of the iron additives. While the addition of $FeCl_3$ led first to the formation of black iron sulfide (FeS), which subsequently oxidized to orange Fe(III) hydroxide, no optical change of the granulated iron hydroxide was visible. The reaction time depended on the type and amount of additive: When using the Fe(III) hydroxide the reaction took longer but could be enhanced by increasing the amount of added particles. The reaction with $FeCl_3$ was very fast and completed in less than 20 minutes. In both cases (addition of $FeCl_3$ solution - and granulated iron oxide) the pH was constantly rising from about 6.3 to 7.5 during the reaction, which was explained by loss of protons due to purging out of the gaseous H_2S. The redox value, which was measured over time, remained constant after addition of granulated iron oxide (about -350 mV), but strongly increased from -350 mV to -50 mV after adding the $FeCl_3$ suggesting a strong electron consuming reaction. This was explained by a two-step reaction: First, the Fe(III) was reduced to Fe(II) by oxidation of either sulfide or thiosulfate to sulfate. Afterwards, the Fe(II) oxidized again by dissolved oxygen forming orange Fe(III) hydroxides.

The filtration of the suspensions containing granulated iron hydroxide as additive by using a reversible flow filter at a mesh size of 5 µm, all particles could be removed from the system thus obtaining clear, H_2S free solution. For the solutions reacted with $FeCl_3$, however, smaller mesh sizes were needed to remove all particles. This study demonstrated that by Fe(III) addition into geothermal brine containing hydrogen sulfide, the sulfide can be successfully removed from the aqueous phase within a short time.

Table of Content

1 Introduction

Many geothermal waters contain the toxic and corrosive gas hydrogen sulfide (H_2S). Geothermal operators need solutions to deal with this component not only due to its toxic and corrosive properties but also because of its strong smell that is already detectable by the human nose in small concentrations. Examples of H_2S containing geothermal waters are known from all over the world, especially form volcanic affected brines such as those in Iceland (Kristmannsdóttir, 2005), or Indonesia (Nasution et al., 2000), but also in carbonate aquifers of the South German Molasse Basin (Mayrhofer, et al., 2014).

H_2S is an ubiquitous gas in the environment. It not only occurs in volcanic gases (Hansell & Oppenheimer, 2004) or together with natural methane as sour gas (CH_4 + H_2S), but it can also be produced in soil and ground water by sulfate-reducing microorganisms that decompose organic matter in the absence of oxygen (O_2; anaerobic digestion). In general, H_2S forms when elemental sulfur (S_0) comes in contact with organic material, especially at high temperatures Berner (1985).

Sulfur (S_0) and sulfate (SO_4^{2-}) -reducing bacteria derive energy from hydrogen or organic molecules by reducing sulfur or sulfate to hydrogen sulfide in the absence of oxygen (O_2). At low oxygen conditions organic matter decays and sulfate-reducing bacteria will use the sulfate present in the water to oxidize the organic matter, by producing hydrogen sulfide as waste. The hydrogen sulfide can react with aqueous metal ions to produce hardly soluble, dark colored metal sulfides such as ferrous sulfide (FeS, FeS_2). Thus hydrogen sulfide can be present naturally in all types of waters that are depleted in oxygen.

H_2S only slightly dissolves in water at ambient conditions and only small proportions dissociate (H_2S+ H_2O → HS^- + H^+ thereby forming a weak acid with a pk_a of 6.9). According to recent investigations by Raman spectroscopy, in aqueous solutions only HS^- and no S^{2-} anions are present (May et al., 2018). At pressures above 18 bar H_2S remains dissolved in water.

Due to the affinity of sulfide for iron, hydrogen sulfide is poisonous for the human body, because it binds to iron in the mitochondrial cytochrome enzymes, thus preventing cellular respiration and

damaging especially the nervous system. While it is harmless at lower concentrations (< 5 ppm), when the human body is able of detoxification processes by oxidizing sulfide to sulfate already at 20 ppm damages of the cornea have been reported (Reiffenstein et al., 1992). The lethal threshold is about 300 to 350 ppm, when the oxidative enzymes become overwhelmed (Ramasamy et al., 2006). Besides its toxic effect and the unpleasant smell, it can also be responsible for deterioration of materials causing severe corrosion damages (sulfide stress corrosion cracking) an effect that is also strongly enhanced by microorganisms (biogenic corrosion; Jia et al., 2018).
Many processes have been designed to remove hydrogen sulfide from drinking or geothermal water such as chlorination (e.g. addition of hypochlorite that oxidizes the sulfide to solid S_0), aeration (oxidation to sulfate at low concentrations); or nitrate addition (Baldacci et al. 2005).
This study suggests to add Fe(III) compounds into H_2S bearing waters. The hypothesis is that Fe(III) will be reduced to Fe(II) and the sulfide precipitates as iron sulfide (FeS or FeS_2) or oxidizes further to the less toxic sulfate (SO_4^{2-}).
The following reactions can be assumed to happen in those H_2S containing systems: In sulfide and Fe(III) containing solutions, sulfide can act as electron acceptor and reduce the Fe(III) to Fe(II), while being oxidized to sulfate (SO_4^{2-}; eq. Ia, Ib, Ic):

$Fe^{3+} + e^- \rightarrow Fe^{2+}$ (Ia)

$HS^- + 4H_2O \rightarrow SO_4^{2-} + 8\ e^- + 9\ H^+$ (Ib)

The two half reactions Ia and Ib together result in

$8\ Fe^{3+} + HS^- + 4\ H_2O \rightarrow 8\ Fe^{2+} + SO_4^{2-} + 9\ H^+$ (Ic)

At reducing conditions, the formed Fe(II) can subsequently precipitate with sulfide to solid iron sulfide such as FeS (pyrotite; II) or, by further oxidizing the sulfide from the oxidation state of -2 to -1 in FeS_2 (pyrite, marcasite; III):

$HS^- + Fe^{2+} \rightarrow FeS + H^+$ (II)

$2\ HS^- + Fe^{2+} \rightarrow FeS_2 + 2H^+ + e^-$ (III)

Whereas in the presence of oxygen, both sulfide and Fe(II) can be oxidized to sulphate and Fe(III), respectively (eq. IV and V).

$H_2S + 2O_2 \rightarrow SO_4^{2-} + 2H^+$ (IV)

$2Fe^{2+} + O_2 + 4H_2O \rightarrow 2Fe(OH)_3 + 2H^+$ (V)

With $Fe(OH)_3$ representing all kinds of iron(III) hydroxides such as goethite (FeOOH), ferrihydrite (Fe_2O_3*$0.5H_2O$), etc.
In this study it is hypothesized that when Fe(III) is added to the thermal waters either as solid iron hydroxide or as a solution of $FeCl_3$, it can be reduced by the sulfide (eq. II and III), while simultaneously acid will be consumed (eq. VI):
$Fe(OH)_3 + 3H^+ + e^- \rightarrow Fe^{2+} + 3H_2O$ (VI)
The formed sulfate (eq. II) can also be bound directly to the solid iron(III) hydroxide by specific adsorption, which is especially efficient in acid environment (Cornell & Schwertmann, 2003; eq. VII):

$SO_4^{2-} + Fe(OH)^{2+} \rightarrow \equiv Fe\text{-}SO_4 + 2OH^-$ (VII)

With "≡" representing the iron oxide surface group.

It should be noted that by air oxygen only small amounts (< 2 mg/L) of H_2S can be oxidized to sulfate and the kinetics of H_2S oxidation are relatively slow (Kovalenko et al., 2001). Based on these assumptions, the removal of sulfide by Fe(III) addition seems likely. However, these reactions can be affected by other ions in solution especially oxygen, carbonate, the pH, temperature and the presence of microorganisms.
The PERFORM project investigates if it is possible to remove H_2S from the geothermal brine. In

detail, the aim of this study was (i) to test the above described method with two different Fe(III) species directly at a geothermal site, (ii) to quantify and (iii) to determine the kinetics of the reactions.

2 Materials & Methods

2.1 Site description

The thermal bath Oberlaa is located in a Southern suburb of the city of Vienna. Its thermal water is used for heating the recreation area, which hosts up to two thousand people per day. Vienna is geologically situated in the Vienna Basin, a large sedimentary basin structure in central Europe stretching in SW-NE direction between the Alps, the Carpathians and the Pannonian Plain. Sedimentary layers of Miocene age deposited in the basin that reach a maximum thickness of 5500 m (Goldbrunner, 2010). In the area of the Vienna basin several geothermal sites have been developed, most of them serving as spas but at the site Bad Blumau additionally also electricity and heat are produced (Legman, 2003). At Oberlaa, two geothermal wells have been drilled (TH1 and TH2) into a fault system at 364 m producing water with 53 °C (Zötl, 1997). Waters are of moderate salinity (3-4 g/L) dominated by Mg, Ca, SO4, and Cl. Highly variable sulfide concentrations have been observed ranging between 13 and 46 mg/L (unpublished reports).
Currently the operators add sulfuric acid and sodium hydroxide to the thermal water to clean it from H2S and use it for bathing. In a first step, the thermal water is degassed by air stripping and addition of sulfuric acid, which removes the H2S together with CO2 gas from the water. The H2S enriched air flows over an absorber which is contains sodium hydroxide thus binding the gaseous H2S to the aqueous phase again. The formed fluid mixture is then disposed to the sewage water and desulfurized water is filtered over a gravel filter to remove precipitated gypsum and to eventually use the conditioned thermal water for bathing. The gravel filter has to be flushed back regularly and the backwash is also collected as sewage water in a retention pool. The back wash water and water from the conditioning steps lead to large scale gypsum and carbonate precipitations. Since the use of chemicals such as sulfuric acid and sodium hydroxide is expensive and the use of hazardous substances is unwanted, it is of interest to investigate alternative methods to reduce the sulfide content of thermal water.

2.2 Experimental set-up

Experiments were performed between the 18th and 20th of June 2019. A one cubic meter plastic container (IBC) was connected to the wellheads. Always a 1:1 mixture from both wells, TH1 and TH2 was obtained. The produced water would flow first into the IBC reaction container, where the additive could be injected. Two different Fe(III) components were tested:

- Granular ferric hydroxide (GFH): This fine grained, dark brown, weakly crystalline and porous iron hydroxide is a synthetically produced mixture of akaganeite (β-FeOOH; 50-70 %), ferrihydrite, and other iron oxides with 43-48 % water (Bahr, 2012). GFH is often used as a selective adsorbens for the removal of heavy metals in drinking- and waste water treatment. Typically, GFH with a grain size of 0.2-2 mm is used for filter systems. In this study however, the fraction <0.2 mm was used achieve better suspension and improved mixing of the particles in the reaction container. 1 ml GFH corresponds to a dry mass of 0.51 g. According to the product data sheet the surface area of GFH determined using the BET method is 300 m^2/g.
- $FeCl_3$ stock solution (40 %): The dark red, highly acidic solution is of p.a. grade. It was directly added to the Reaktion container.

The reaction container was equipped with a stirrer to enable quick and homogenous mixing. Additionally, an air compressor was connected to allow good mixing of the water with air oxygen. A flow through cell containing a set of electrodes (pH, redox, electric conductivity, and dissolved

oxygen) was installed at the outlet of the reactor. Via an opening in the container lid, the additives could be injected into the reaction container (Fig 1).
From the reaction container the brine would flow first through a filter ("HydroGeoFilt"). This self-cleaning filter was recently designed and developed for use at geothermal sites (patent is to come) system is adapted to high temperature and pressures (e.g. thermal water). In total five filter candles with different mesh sizes (here: 5, 10, 25, 50 and 100 µm) can be installed (Fig 1 C). During backwashing an ultrasonic device installed in a stainless steel case removes the filter cake from the filter candles. After the thermal water has passed through the filter unit, it enters a measurement device that measures every minute pH, redox (Eh), electric conductivity, density, and temperature (Fig. 1, D) FluMo-1, Milsch et al., 2013, Feldbusch et al., 2013). From the FluMo outflow (E), the water was either discarded into the sewage system or connected to the IBC container to ensure circulation of the fluid. Sample collection was possible at E or directly from the IBC container (Fig. 1).

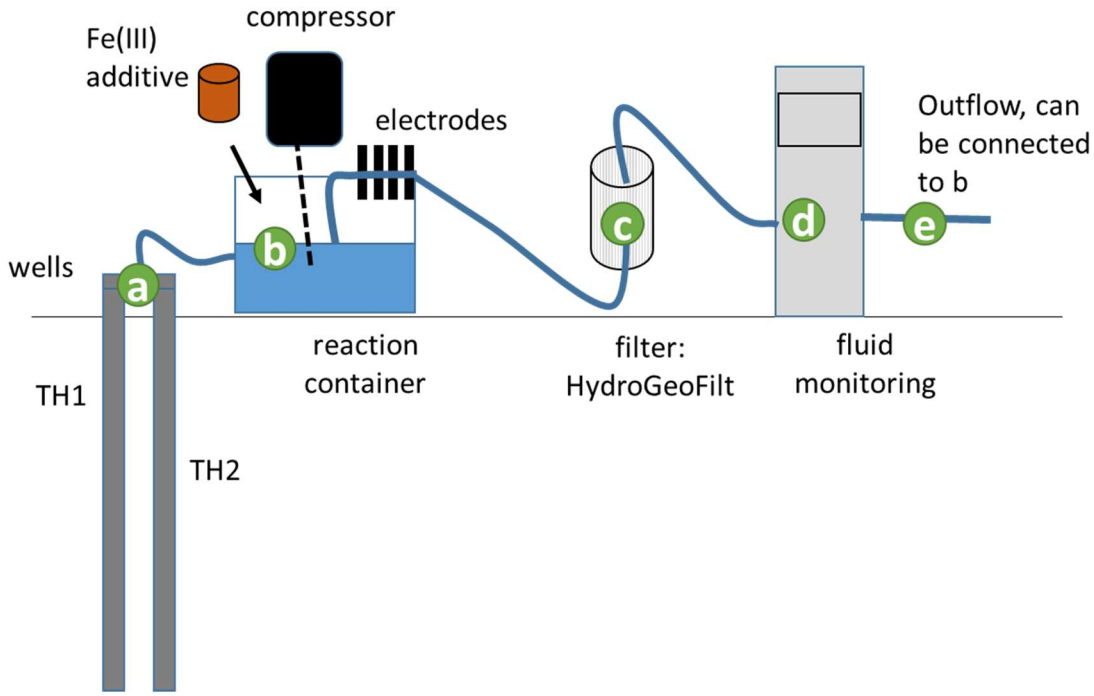

Fig. 1: Experimental set-up: The fluid flows from the two connected wells (TH 1 and 2; a) first into the reaction container (b), where the Fe(III) additive can be injected and an air compressor is connected to. At the outlet pH, redox, dissolved oxygen (DO) and electric conductivity are measured. After passing through the filter (c), the same parameters were measured in a monitoring device (d).

Before the actual experiment started, three pre-tests were conducted at the site to better define the system:

Pre-experiment I: To test the **variability and ranges of chemo-physical parameters of the geothermal brine** over time each 2 l water were collected directly from the wells (A) and the parameters were immediately measured by the same probes as those used in the IBC reaction container. This was repeated five times over 20 minutes and mean values and standard deviation were determined to obtain a baseline of the thermal water for pH, redox, electric conductivity, and DO.

Pre-experiment II: Addition of GFH to the thermal water **to estimate the speed of the reaction:** 0.5 mL GFH was added to 400 mL fresh thermal water taken directly from the well at location A (corresponds to 0.64 g dry mass GFH/L water). Seven sub-samples were collected over a period of 30 minutes and sulfide was measured photometrically (see 2.3) therein.

Pre-experiment III: Experiment to **determine the minimum amount of $FeCl_3$** to be added to the thermal water to bind all sulfide: Since the $FeCl_3$ stock solution (40 % or 4 M) reacts highly acidic (pH < 0) a strong dissolution with thermal water was needed to guarantee on the one hand side a neutral pH value but to obtain on the other hand a sufficient amount of Fe for removing all solution sulfide: Various ratios of $FeCl_3$ solution and thermal water were prepared (1:100, 1:1000, 1:10000) and pH value and sulfide were measured immediately after mixing the two together.

Large scale flow through experiments

The following experimental settings (in chronological order) were tested based on the experimental Set-up, shown in figure 1 (table 1): In all experiments, pH, redox (Eh), dissolved oxygen (DO), electric conductivity (EC), and temperature were measured directly in the reaction container. Filtering and subsequent fluid monitoring was only done in experiments B, C, D, and E. Sample collection occurred either in the container or after the fluid monitoring device. During experiment A, the thermal water just circulated in the reactor and GFH was added in access. In experiment B, also the filter and the fluid monitoring behind were connected. In experiment C, again only in the reactor was measured but this time also the effect of the compressor bubbling air into the reactor was tested and the amount of GFH was reduced and added in two steps (each 0.1125 g/L).

Table 1 Experimental setting and amount used additives (GFH or 40 % $FeCl_3$ solution).

Experimental setting	Type and amount of additive per volume thermal water	Filtered & monitored
A_0 (no compressor)	0	-
A_1	500 mL GFH in 300 L (0.85 g/L)	no
B_0 (no compressor)	0	-
B_1	500 mL GFH in 300 L (0.85 g/L)	yes
C_0_1 (no compressor)	0	-
C_0_2 (compressor)	0	-
C_1_1 (compressor)	55 ml GFH in 300 L (0.094 g/L)	yes
C_1_2 (compressor)	55 ml GFH in 300 L (total 0.187 g/L)	yes
D_0 (compressor)	0	yes
D_1	50 mL GFH in 400 L (0.06 g/L)	yes
E_0 (compressor)	0	yes
E_1	75mL $FeCl_3$ in 400 L	yes

2.3 Analytical methods

2.3.1 Field analysis

Sulfide was measured photometrically (Multilab P5) after acidifying the samples because in the acidic range, the sulfide species H_2S, HS^-, and S^{2-} practically all occur as aqueous hydrogen sulfide (HS^-) and react with dimethyl-p-phenylenediamine and Fe(III) ions to methylene blue (Cline, 1969). This colored complex is measured at a wavelength of 665 nm. The thickness of the cuvette was one cm and the maximum dilution of the thermal water was 1:20. The measurement accuracy is ± 0.017 mg/l.

Fluid physical parameter (electric conductivity (EC), pH, redox, and dissolved oxygen (DO)) were measured in a flow through cell directly at the outflow of the IBC container by electrodes (DO amperometrically, the pH by glass electrode, redox by Ag/AgCl probe). Values were recorded every few minutes thus giving punctual information. The fluid monitoring System, FluMo, installed after the HydroGeoFilt measures the same physicochemical parameters also in flow-through cells but collects data every minute and stores them automatically thus giving a much higher accuracy.

To estimate the grain sizes of particles before and after the reaction with the thermal brine, three filters were connected with a tube to each other in a row (cascade filter, Fig 2) and about 500 ml

brine with either $FeCl_3$ or with GFH additive were injected with a syringe to the line. Only visually it was estimated after which step the particles were removed. Altogether four of those tests were performed at the site.

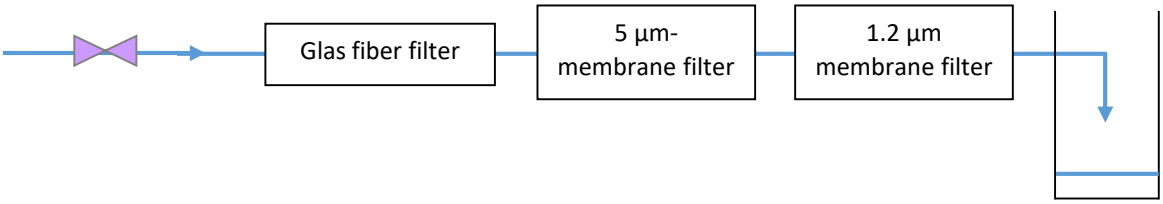

Fig. 2: Scheme of cascade filtration to estimate the grain size distribution of the solid phase in the system.

2.3.2 Laboratory analysis

Cation and anion concentrations were measured with a Thermo Sientific Dionex ion chromatography system and evaluated using the Dionex Chromeleon 6.8 software.
The organic content was characterized in four samples by ion chromatography (for organic acids) and liquid chromatography organic carbon detection (LC-OCD) (for size distribution of the molecules). Two of the selected samples were collected in untreated water directly from the well, one was collected after treatment with GFH (experiment C) and one after treatment with $FeCl_3$ (experiment D).
Precipitates as collected from the filters were analysed for their mineral composition by X-ray diffraction (XRD; with a Cu Kα1 radiation source and primary monochromator; Table 2). Diffractograms were semi-quantitatively evaluated by the software EVA. Scanning electron microscopy (SEM) with a beam current acceleration of 20 kV, and a maximum aperture of 120 µm was applied on four of the filter residue samples. On selected image spots, the material composition was semi-quantitatively characterized by energy dispersive X-ray (EDX), using the same accelerating voltage (Table 2).

Table 2 Selected samples for solid phase analysis (XRD and SEM).

Nr	Experiment description	XRD	SEM
1	experiment D; filter backwash 5+10 µm	y	y
8	Filter test 2 ($FeCl_3$); 5 µm filter	y	y
9	experiment E; Filter test 3; 5 µm $FeCl_3$; 100µL; 400mL TH 1+2	y	n
10	Filter test 4 ($FeCl_3$); 1.2 µm; taken from IBC	n	n
11	Filter test 4 ($FeCl_3$); 5 µm filter; taken from IBC with	y	y
2	experiment E; filter backwash 10 µm	y	y
3	experiment E filter backwash 5 µm;	y	y
12	Pre experiment $FeCl_3$:TH 1:10000 pH=6.9	y	n

3 Results

3.1 Pre-experiments

Pre-experiment I:
The thermal water without addition of any additives has a temperature of about 50 °C and is of neutral pH-value (6.5). The EC is relatively low (4.8 mS/cm) but above freshwater and conditions are strongly reducing (-372 mV; table 2). Altogether, these values were relatively stable over time as confirmed by their low standard deviations resulting of five measurements over 17 minutes (Table 3).

Table 3: Background values of physico-chemical parameters of the thermal water (mean values and standard deviation of five measurements over 17 minutes).

	pH	EC (mS/cm)	Eh (mV)	DO (mg/L)	T (°C)
Mean value thermal water	6.51	4.80	-372.95	0.17	49.80
Standard deviation	0.005	0.000	3.708	0.027	0.173

Pre-experiment II:
After adding GFH to thermal water in a beaker, the sulfide content decreased from 30 to almost 0 mg/L in less than 20 minutes (Fig. 3). Assuming a first order reaction ($Fe^{3+} + S^{2-} \leftrightarrow FeS$), the rate constant, in a 0.78 g/L suspension as given from the slope is 1.7 mg sulfide consumption per minute (Fig.3).

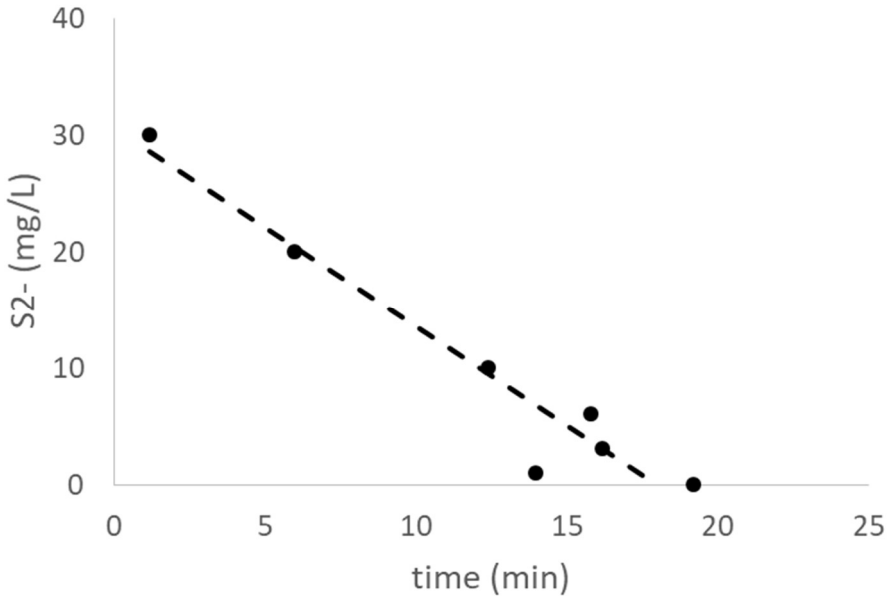

Fig. 3: Sulfide concentration measured over time after GFH was added into a glass beaker filled with fresh thermal water (0.64 g/L).

Pre-experiment III:
Dilutions of $FeCl_3$ solution (40 %) with fresh thermal water and with aged thermal water (sulfide already removed) were tested in different ratios and the pH and the sulfide concentration (for pH >6) was measured. In 400 ml thermal water with 50 µL $FeCl_3$, the solutions turned immediately black, the same happened with 100 mL thermal water and 100 µL $FeCl_3$ (Table 4). After filtration (0.45 µm) all these solutions became clear again.

Table 4: Pre experiment III: mixing a 40% $FeCl_3$ solution with thermal water in different ratios.

Mixing ratio*	Fe added (mg/L)	pH	remark	Sulfide (mg/L)
1: 100	2000	1.3	red	nm
1: 1000	200	2.8		nm
1:10000	20 (0.4 mM)	6.9		nm
1:4000	50	6.1	Black	2.2
1:8000	25	6.17		5

Assuming the reactions eq. IIIa or b, to oxidize a sulfide concentration of about 1 mM (32 mg/L), as measured in the thermal water, either 1 or 0.5 mM Fe would be. Based on the dilution test and this assumption, it was decided to add for the actual experiment 75 ml of the $FeCl_3$ solution into the IBC container with 400 L thermal water to obtain a mixing ratio of 1:5333 corresponding to 37.5 mg Fe/L at a pH of 6.1.

3.2 Main experiments

3.2.1 In situ parameters

Addition of GFH to thermal water

When circulating fluid from the well through the IBC container (e.g. experiment C), the pH remained relatively stable (6.65) while redox and oxygen decreased slightly. After switching on the compressor, more air oxygen entered permanently the water and redox, pH, and oxygen increased (Fig.3). The addition of GFH (0.125 g/L Fe) resulted in a decrease of the redox, DO, and sulfide (from 21 to 14 mg/L), while the pH continued to increase (up to pH 7.6). When the sulfide concentration stabilized at around 14 mg/L, DO and redox slightly increased again. At this point, the same amount of GFH was added again and the sulfide decreased further to 7.9 mg/L. After another 40 minutes a last sample was collected that showed a sulfide concentration below detection limit (Fig. 4).

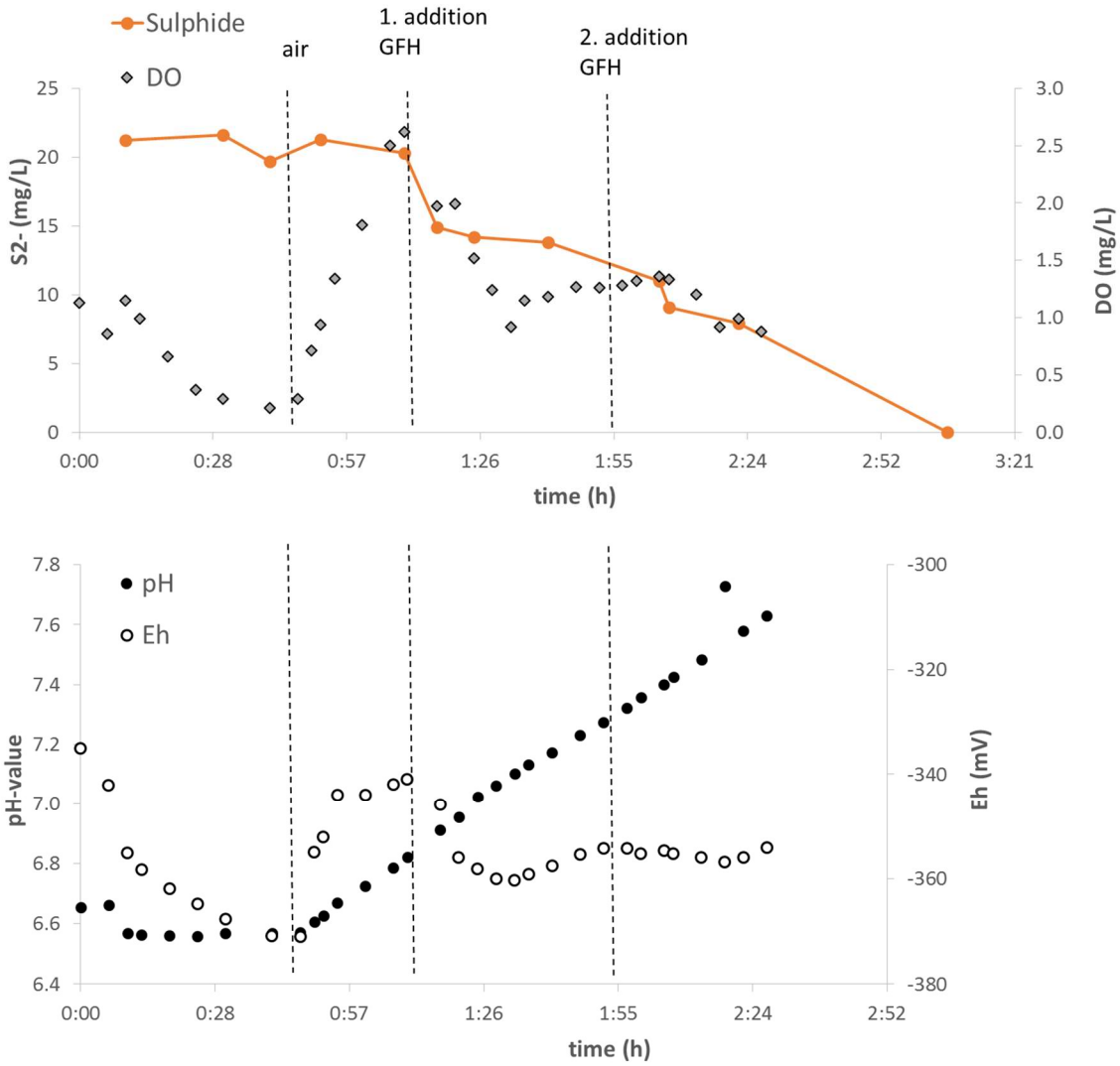

Fig. 4 Change of sulfide, DO (top) and redox and pH- value (bottom) over time in dependence of the experimental conditions (experiment C), measured in the outflow of the reactor. GFH was added twice as marked in the diagram.

Similarly, during experiment D, GFH was added to the IBC container. This time the HydroGeoFilt and afterwards the fluid monitoring system was connected to the fluid loop (Fig.1). Again it was found that the pH-value constantly increased as soon as the air compressor was switched on (from 6.9 to 7.4), whereas the redox was relatively constant between -339 and -344 mV. Once GFH was added to the system, sulfide started decreasing, a process that took about 30 minutes until GFH was fully removed.

Before adding GFH, the fluid monitoring device started measuring the fluid physical properties of the thermal water. Similar to measurements in the container, the pH increased (from 7.5 to 7.9) and the redox remained constant (-337 mV). When GFH was added, the fluid monitoring with FluMo had to be stopped and was switched on again after 14 minutes. During this time, the pH and redox first increased and decreased again until both values stabilized after around 40 minutes. This is about the same time it took until all sulfide was removed from the system. The monitored parameter (pH and Eh) proved to be very sensitive, as obvious by glitches in both curves, when filter candles were changed (Fig. 5).

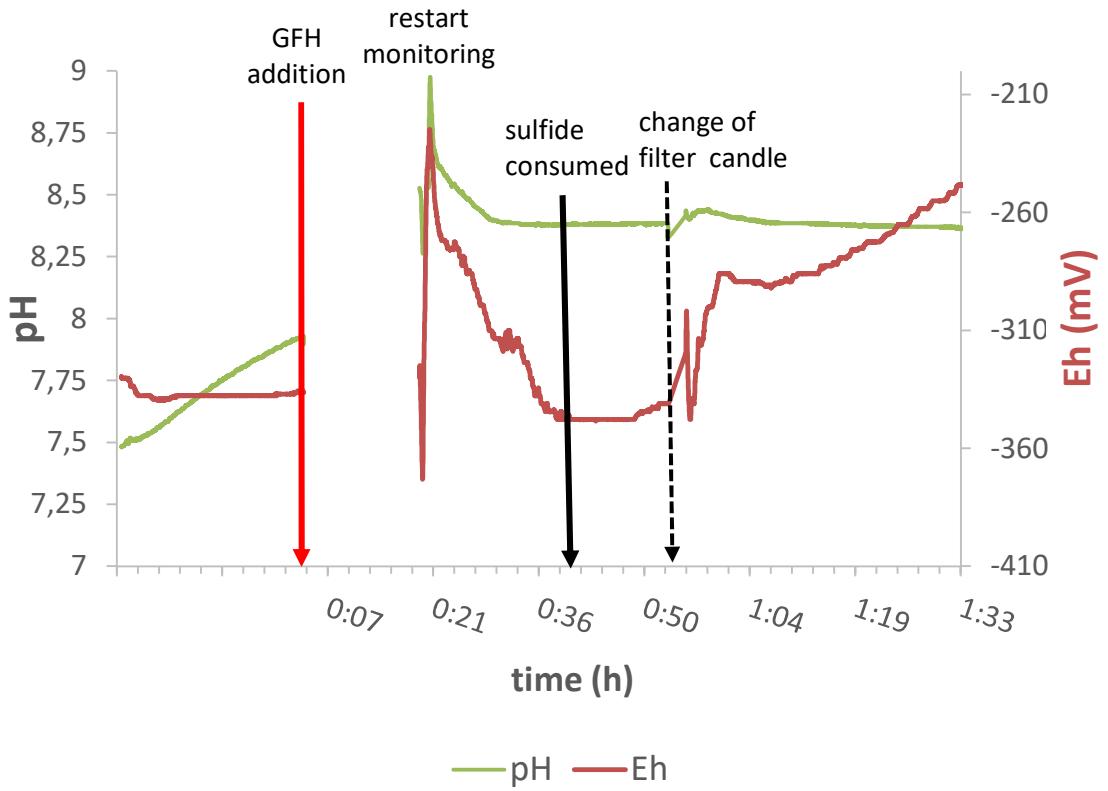

Fig. 5 pH and Eh monitoring by the fluid monitoring device FluMo during experiment D after the filter.

Addition of $FeCl_3$ solution

The addition of concentrated $FeCl_3$ solution into the IBC container (Experiment E) resulted in an immediate color change of the fluid (from colorless to black) and the complete removal of sulfide in the IBC container after 17 minutes (Fig. 6). After about 30 minutes, the color of the fluid in the IBC container changed from a homogenous black solution via grey to orange (Fig. 7).

Over time both, pH and Eh increased. Similar as compared to the experiments with GFH, the pH value further increased even after all sulfide was consumed. The redox increased more strongly (up to -50 mV) both, in the IBC container (Fig. 6) and when measured after der filtering with FluMo (Fig. 7).

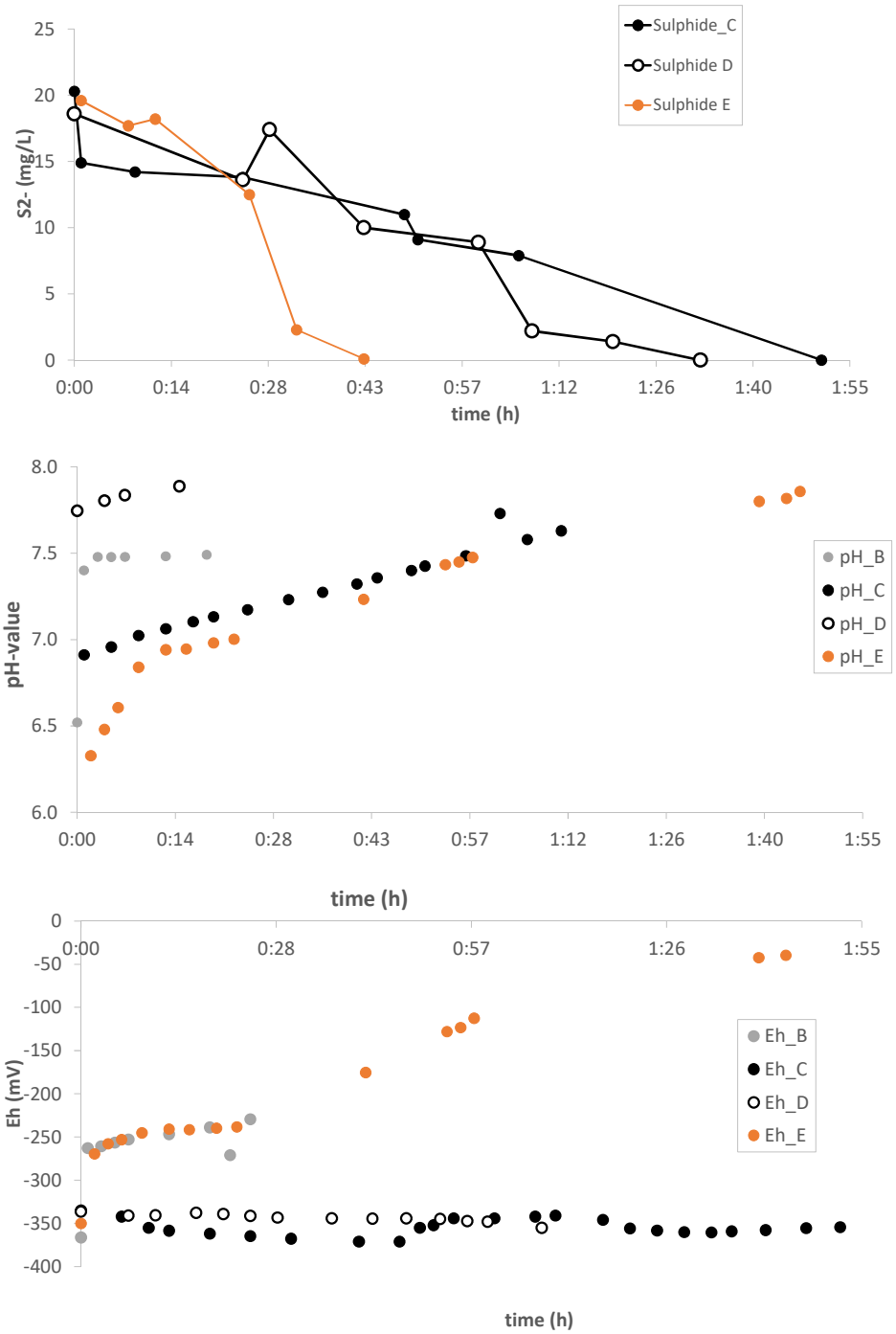

Fig. 6 Concentration of hydrogen sulfide (top), pH value (middle), and redox (bottom) in the reaction container after adding GFH (B, C, D) and $FeCl_3$ (E: orange dots) to the thermal water.

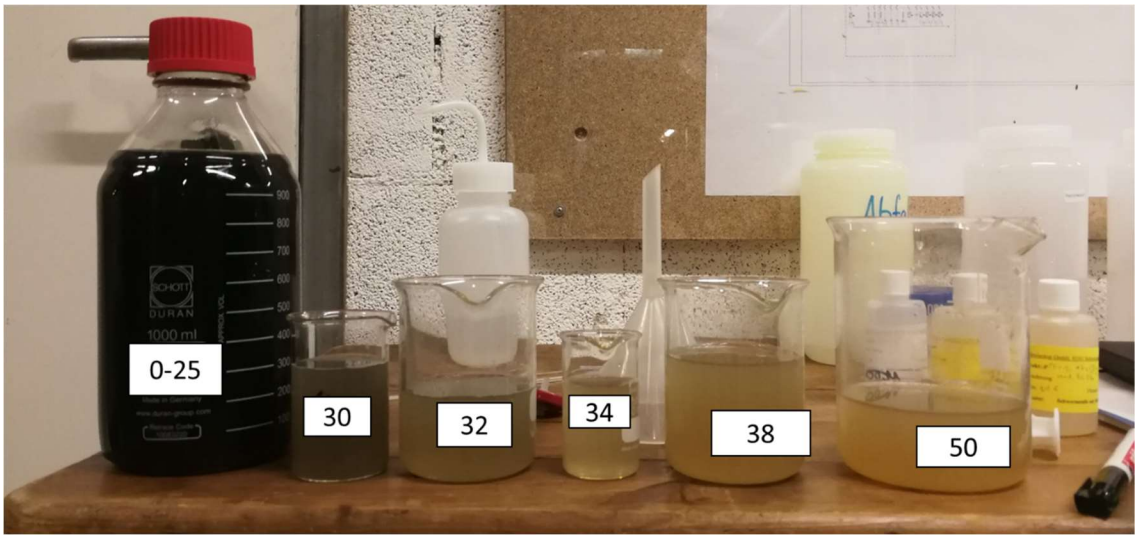

Fig. 7 Color change of the thermal water collected from the reaction container after addition of $FeCl_3$ (experiment E). Numbers indicate sample collection in minutes after $FeCl_3$addition.

Similarly, the measurements of fluid parameters behind the filter showed an increase of redox over time after addition of $FeCl_3$ solution to the thermal water (Fig. 8). After all sulfide was removed from the solution, the redox dropped and only afterwards it rose again (Fig 8).

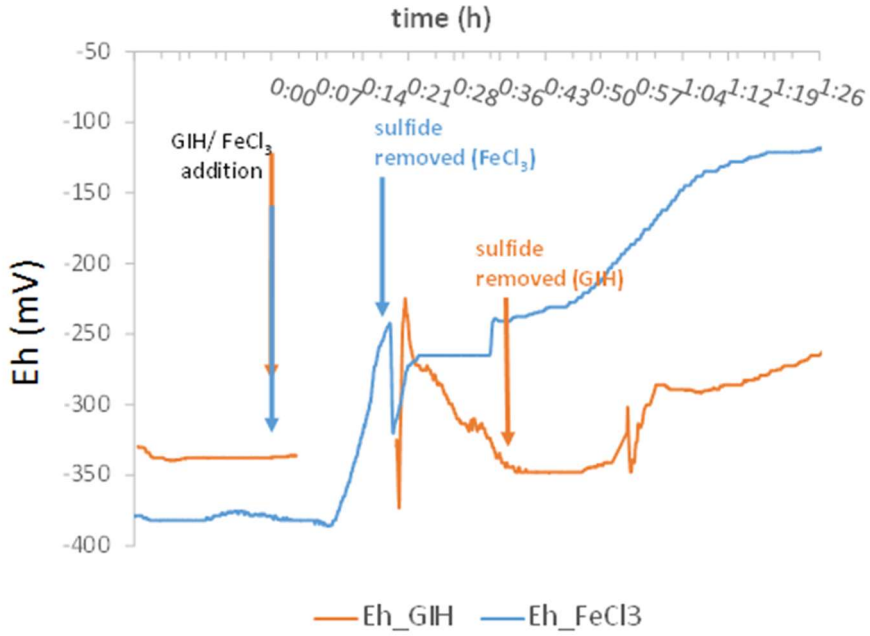

Fig. 8 Change of Eh as measured by the fluid monitoring device FluMo after filtration of the thermal water in experiment D (addition of GFH) and experiment E (addition of $FeCl_3$).

3.2.2 Lab analysis: water chemistry

Analysis of the elemental composition

Results of the elemental composition of selected water samples are given in table 5. The anions of the thermal water are composed mainly of chloride (830-880 mg/L) and sulfate (1600-1200 mg/L),

which both hardly changed in dependence of the type and duration of the experiment. Since sulfate showed no specific behavior in dependence of the amount and type of iron additive, apparently the formed amount of sulfate by Fe(III) reduction was still in the same order of magnitude as compared to the variability of sulfate composition of the brine. Similarly, Mg, Ca, and K concentrations showed no treatment –dependent variability being in the range of 100-120 mg/L, 400-430 mg/L, and 20-22 mg/L, respectively (table 5). Manganese was below detection limit and the alkalinity ranged between 14.6 mM and 15.6 mM). Solely the iron concentration varied more strongly between below detection limit (< 0.02 mg/L) and 10.5 mg/L. In three samples, a high iron concentration was measured (table 5).

Table 5. Main cations and anion of selected water samples during different experiments (mg/L).

Sample	treatment	Na^+	K^+	Ca^{2+}	Mg^{2+}	HCO_3^-	Cl^-	SO_4^{2-}	Fe
water	filtered	520	23	430	130	172	860	1400	<0.02
water	unfiltered	510	22	420	130	233	800	1300	<0.02
Exp. C	Before addition	510	22	430	120	nm	nm	1500	<0.02
	After GFH_1	510	22	430	120	nm	nm	1500	4.5
	After GFH_2	510	21	420	120	nm	nm	1500	10.5
	After GFH_2	510	22	430	120	nm	nm	1500	<0.02
Exp.D	Before addition	480	21	400	120	nm	nm	1500	<0.02
	Before addition	480	20	400	110	nm	nm	1400	<0.02
	After GFH	480	20	400	110	nm	nm	1400	<0.02
	After GFH	450	18	350	100	nm	nm	1200	<0.02
	After GFH	460	19	370	110	nm	nm	1300	<0.02
Exp E	Before addition	510	22	430	120	nm	nm	1500	<0.02
	After FeCl3	530	21	420	120	nm	nm	1400	6.7
	After FeCl3	510	22	420	120	nm	nm	1500	<0-02
	After FeCl3	510	22	430	120	nm	nm	1400	<0.02
	After FeCl3	510	21	420	120	nm	nm	1400	2.186

nm: not measured

The anion thiosulfate ($S_2O_3^{2-}$) was measured in two samples of the untreated thermal water (24 - 30 mg/L) and in two samples of GFH and $FeCl_3$ treated samples. A clear decrease of thiosulfate was measured after the addition of both additives. However, it was less complete after adding GFH (4.6 mg/L remaining) and almost fully complete after adding $FeCl_3$ (0.8 mg/L thiosulfate).
Measurements of the organic composition of the thermal water indicated that no measurable amounts of organic acids were present in the samples. The organic carbon content ranged between 0.2 and 0.4 mg/L in all samples. The addition of $FeCl_3$ or GFH showed no evident effect on organic carbon content.

3.2.3 Lab analysis: Solid phase

Selected samples from either the backwash of the HydroGeoFilt or from the cascade filters tests were analyzed by either XRD and/or SEM (table 2). The cascade filter test indicated that for suspensions containing GFH, particles were relatively large and all visible particles were retained at filter size 1.2 µm. Indeed, those water samples were also clear when filtered by the HydroGeo Filt using mesh size <10µm. However, when applying the $FeCl_3$ method, formed particles were smaller than the smallest used filter size (HydroGeoFilt: <5 µm; cascade filter < 1.2 µm). However, by filtration with a 0.45 µm syringe filter, also those water samples became clear.
XRD analysis of the filter residues either from the cascade filter tests of from the HydroGeoFilIt, all derived from the reaction of $FeCl_3$ with thermal water revealed the presence of weakly crystalline substances as indicated by the high background noise (Fig. 9). All measured samples hardly differed

with respect to their mineral composition. The identification of the few peaks indicated the presence of pyrothite (Fig. 9). No interpretation was possible for the other peaks.

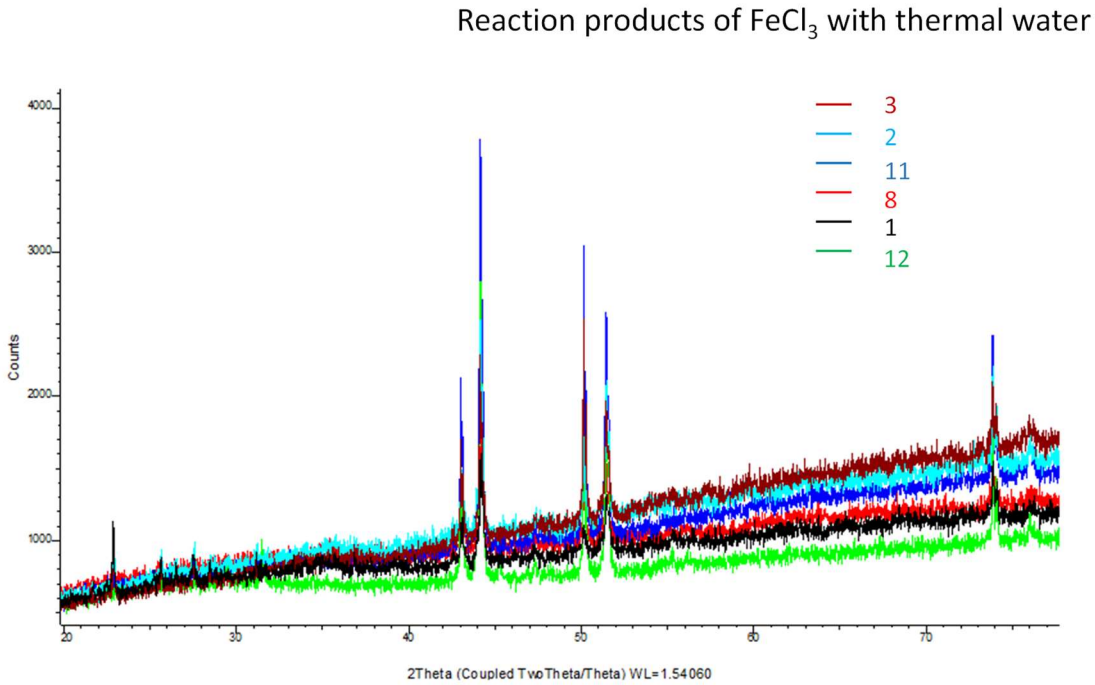

Fig. 9: XRD pattern of iron precipitates collected from the filters (see table 2).

Scanning electron micrographs of the formed particles collected from the filters showed few samples that exhibited clear crystalline structures. By application of EDX mainly four oxides were detectable: SO_3, Fe_2O_3, CaO, and SiO_2. The few crystalline particles could be attributed to gypsum (consisting mainly CaO and SO4) indicating that by drying (water evaporation) gypsum saturation was reached. Samples from experiment D and consisted to similar ratios out of the elements S and Fe. In experiment E, however, the Fe fraction was much more variable and also higher (up to 80-90 % Fe_2O_3; Fig. 10).

Filter residue (backwash, 5+10 µm) experiment D (sample 1)

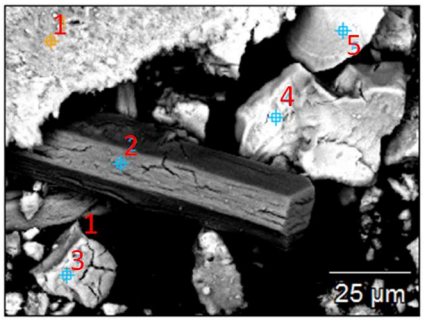

	SO3	SiO2	CaO	Fe2O3
1	55.73	6.22	10.79	23.94
2	58.18		40.80	1.01
3	37.74	4.26	0.25	55.38
4	36.30	2.03	0.74	59.71
5	45.97	4.22	0.41	47.98

Filter residue (backwash 10 µm) experiment E (sample 2)

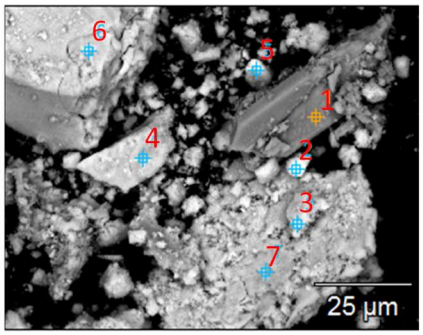

	SO3	SiO2	CaO	Fe2O3
1	48.34	1.78	39.69	4.61
2	13.41	2.57	1.07	67.42
3	25.27	4.06	0.66	68.37
4	13.23	1.49	0.20	83.97
5	14.74	3.86	1.60	78.20
6	42.36	1.67	0.23	54.23
7	34.75	1.91	0.27	61.35

Filter test 4 (5 µm) from IBC container, experiment E (sample 11)

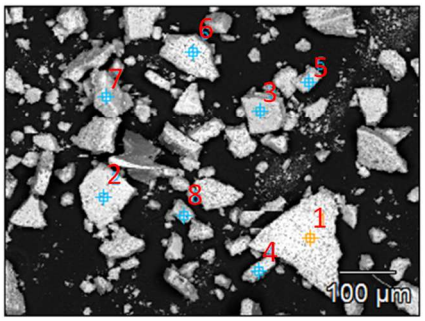

	SO3	SiO2	CaO	Fe2O3
1	16.89	12.78	3.00	60.82
2	16.34	11.96	2.33	64.95
3	10.36	9.64	1.92	74.74
4	15.85	13.81	2.93	62.52
5	8.75	12.35	1.92	71.74
6	14.69	7.59	2.86	70.66
7	13.98	14.48	2.93	64.00
8	50.49	9.46		16.95

Fig. 10: SEM pictures from three samples (see table 2) together with main results from EDX measurements.

4 Discussion

4.1 Processes in the reactor

Sulfur species

Although the geochemical redox system seems relatively simple with just three elements being involved in the reactions (Fe, O, S), various species with several redox states, especially those of sulfur have to be considered to form, party as metastable phases in the reactor. To get an idea, which species are most likely to form, equilibrium calculations were performed with the Hydra/Medusa code (Puigdomenech, 2004), although this program does not consider metastable phases such as thiosulfate. In the pure sulfur water redox system (without iron), at given pH, redox conditions, an oxidation of hydrogen sulfide to sulfate seems likely (Fig 11), whereas elemental sulfur most likely does not form. In the presence of Fe, with increasing redox, the species FeS, FeS_2 and SO_4 are stable. A further increase of the redox to > 5 pe (corresponds to about 30 mV) would have resulted eventually in the formation of a ferric iron oxyhydroxysulfate (Fig. 11).

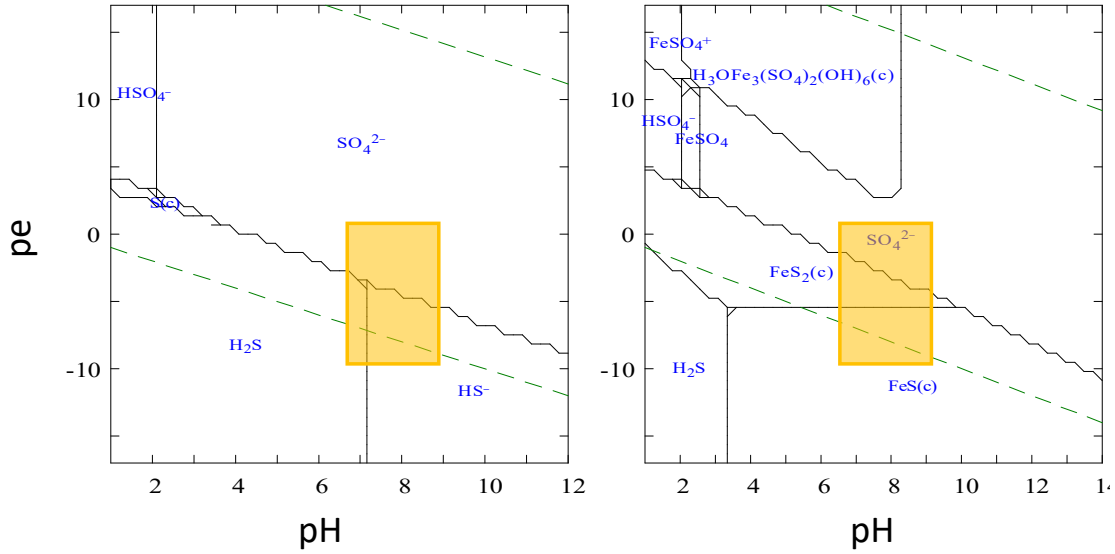

Fig. 11 Predominance diagrams as calculated by the code Hydra/Medusa code (Puigdomenech, for (left) the sulfur redox system and (right), for the iron sulfur redox system at room temperature. Concentrations of Fe and S are each 1 mM. Area of relevance during the experiments is shown in yellow. The redox is given as pe which corresponds to the Eh in V, when multiplied 0.059 at 25 °C.

The system is even more complicated since not only sulfate (SO_4^{2}) and hydrogen sulfide (HS^-, H_2S), occur, but also thiosulfate ($S_2O_3^{2-}$; redox state of S: -2), which was highest in the untreated thermal water samples confirming its natural occurrence in the formation water. The thiosulfate apparently reacted with both of the two iron(III) additives, since it decreased almost completely after the treatments with GFH (down to 4.6 mg/L) and $FeCl_3$ (down to 0.8 g/L).
Thiosulfate reacts with Fe^{3+} to form the metastable aqueous complex ferrous tetrathionate FeS_4O_6 (Druschel et al. (2002).

$2S_2O_3^{2-} + 2Fe^{3+} \rightarrow 2Fe^{2+} + S_4O_6^{2-}$ (VIII)

The product readily decomposes, evolving sulfur dioxide and elemental sulfur:

$FeS_4O_6 = FeSO_4 + SO_2 + 2S$ (IX)

Although it was not possible within this study to verify the presence all these poly sulfur species in the water, their presence is very likely.

Removal of protons
In all experiments (both, with $FeCl_3$ and with GFH, the pH in the IBC container went up over the entire period of the experiments starting with the moment, when the compressor was switched on to pump air bubbles into the water (between 6.3 and 7.8, e.g. Fig. 4 and 6). This increase is explained by a shift in the equilibrium between gaseous and dissolved H_2S. The purging removed more H_2S and therefore more protons from the water and the pH slightly increased. This continued even after all hydrogen sulfide was removed. In the GFH solution the pH even increased further to nearly 9 and decreased afterwards until stabilizing at a pH of 8.5. Based on these results a pH stabilization indicate a completion of the reaction although hydrogen sulfide was consumed already at an earlier stage.

Changes of redox
The redox value did not change significantly when adding GFH to the thermal water, but increased strongly after addition of $FeCl_3$ (Fig 5 and 7). Clearly this strong increase of the Eh value was not only due to dissolution of air oxygen into the thermal water but also oxidation of both, sulfide and thiosulfate by reduction of iron (III) during the formation of the black FeS (eq. 2). This immediate reaction consumed strongly electrons. After the sulfide was removed from the system (experiment E), the Eh decreased again but started to increase afterwards. Simultaneously, the black FeS

oxidized to form an orange iron(III) hydroxide. The sulfide sulfur would also be oxidized but from the present data it cannot be concluded to which redox state. Since thiosulfate also disappeared during the reaction it can be assumed that this was not the final redox state of sulfur. The measured sulfate concentration was generally very high and slightly variable in the system. Assuming about 1 mmol H_2S in the thermal water (32 mg/L), also 1 mmol sulfate (96 mg/L) could have been formed at maximum by reaction with Fe(III). With sulfate ranging between 1200 and 1500 mg/L sulfate in the thermal water even without addition of Fe and values between 1200 and 1500 mg/L after experiments with additives (Table 5), this variations are too large and could not attributed to any reaction-. Therefore most likely sulfur formed during the experiments also some with the applied methods undetectable and unstable phases such as gaseous SO_2 or polysulfides.

Formation of solid phases

Sulfate could also be bound to the surface of the freshly formed iron hydroxide (adsorption) or even form an iron sulfate mineral as well as gypsum ($CaSO_4$*$2H_2O$). Indeed, SEM measurements indicated that gypsum has formed in both, samples from the filter of experiment D and E (with GFH; Fig 10) samples…However, this formation could also be an effect of drying because, as indicated by calculations with PhreeqC (llnl database, data not shown) gypsum saturation was not reached during experimental conditions of this study.

Characterization of the formed solid phases from the $FeCl_3$ solutions as indicated by XRD indicated that pyrothite and another unidentifiable species (unknown XRD peaks) together with weakly crystalline/amorphous iron hydroxides had formed as indicated by the X-ray diffractograms (fig.9). As a metastable phase, also the oxy hydroxyl sulphate schwertmannite seems possible, because it is known to precipitate rapidly upon oxidation of Fe(II) sulphate containing solutions (Regenspurg et al., 2004). However, the pH value of the solutions was most likely to neutral, because schwertmannite typically forms at acidic (< pH 4.0) conditions.

However, many solid, weakly crystalline phases formed in low concentrations are very difficult to detect by most mineralogical methods´. For quantification of those species sequential extraction should be carried out that are suitable for determining also iron sulfides such as pyrite (Müller et al, 2017).

4.2 Kinetics of the reaction

The speed of the reaction depends strongly on the type and amount of Fe(III) added to the system. When using the iron hydroxide GFH at low concentration (< 2.4 mmol Fe or 0.2 g/L, the reaction is relatively slow (6 µmol sulfide/minute will be removed) and stopped after about 0.3 mM (10 mg/L) sulfide were consumed (Fig. 10). This indicates that the GFH surface will not be available for further reaction with the sulfide if not enough surface sites are available. In contrast, when offering a larger amount of iron hydroxide (> 5 mM), the rate of sulfide decrease is rather quickly and complete (0.5-1 mmol/min).

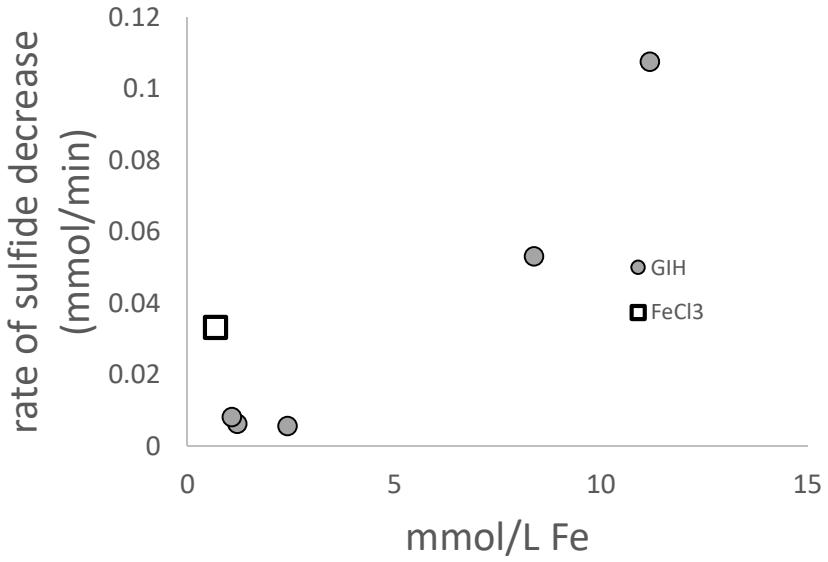

Fig. 10 Rate of sulfide decrease per added amount of iron for all experiments.

When using $FeCl_3$ as additive, the reaction is much faster and less material is needed as additive. By adding only a minimum amount of Fe (0.7 mM), the rate of sulfide removal is at least 0.03 mmol/min. Clearly, the reaction is faster and more complete with this additive. A recycling of the $FeCl_3$ material can also be considered since after the iron sulfide formation, the material would oxidize again to an iron(III) hydroxide, which again can be reused for oxidizing the hydrogen sulfide by being reduced.

5 Conclusions

In this study, it was successfully demonstrated that the suggested method of removing hydrogen sulfide from geothermal brine during operation of a geothermal well by adding Fe(III) is possible. The redox reactions underlying this process are rather manifold due to the different species and redox states the sulfur and iron phases allow. The rates of sulfide consumption vary, depending in the type and amount of added Fe(III). $FeCl_3$ was proven to be much faster to oxidize the hydrogen sulfur. However, when using $FeCl_3$ it has to be considered that moderate concentrations should be used, because otherwise the solution pH is too low and the reduction of Fe(III) to Fe(II) does not take place. Additionally, unwanted reactions such as acid corrosion are likely to occur. Therefore it is recommended to remain in the neutral pH range and keep the $FeCl_3$ concentration constantly at levels that ensure that. In contrast, addition of GFH is not limited by the amount of iron hydroxide added. Since the reaction with GFH is altogether more slowly, higher amounts of this additive are recommended.

The other advantage of addition of $FeCl_3$ in the presence of oxygen is that after oxidation of FeS to Fe(III) hydroxide, the latter material can probably be recycled for further oxidation of hydrogen sulfide. This would save additional costs on material. Another set of field experiments is recommended to be carried out to test this recycling capacity.

Further, the application of the HydroGeoFilt has been proven to be applicable at given geothermal conditions. The filter candles with 5 and 10 µm are sufficient when using the GFH as additive. However, when using $FeCl_3$ as additive, the suspensions yield smaller particles and it is recommended to first test smaller mesh sizes for the filters (e.g. 1-2 µm) before application.

6 References

Baldacci, A., Mannari, M. and Sansone, F., 2005, April. Greening of geothermal power: an innovative technology for abatement of hydrogen sulphide and mercury emission. In *Proceedings of the World Geothermal Congress, Antalya, Turkey* (Vol. 2429).

Bahr, C. 2012. Entfernung von Uran aus Trinkwasser durch Adsorption an granuliertem Eisenhydroxid (GEH). Dissertation, Technical University of Berlin, Faculity 3.

Cline, J.D., 1969. Spectrophotometric determination of hydrogen sulfide in natural waters 1. *Limnology and Oceanography*, *14*(3), pp.454-458.

Cornell, R.M. and Schwertmann, U., 2003. *The iron oxides: structure, properties, reactions, occurrences and uses*. John Wiley & Sons.

Druschel, G.K., Hamers, R.J., Luther, G.W. and Banfield, J.F., 2003. Kinetics and mechanism of trithionate and tetrathionate oxidation at low pH by hydroxyl radicals. *Aquatic Geochemistry*, *9*(2), pp.145-164.

Feldbusch, E., Regenspurg, S., Banks, J., Milsch, H. and Saadat, A., 2013. Alteration of fluid properties during the initial operation of a geothermal plant: results from in situ measurements in Groß Schönebeck. *Environmental earth sciences*, *70*(8), pp.3447-3458.

Hansell, A. and Oppenheimer, C., 2004. Health hazards from volcanic gases: a systematic literature review. Archives of Environmental Health: An International Journal, 59(12), pp.628-639.

Jia, R., Tan, J.L., Jin, P., Blackwood, D.J., Xu, D. and Gu, T., 2018. Effects of biogenic H2S on the microbiologically influenced corrosion of C1018 carbon steel by sulfate reducing Desulfovibrio vulgaris biofilm. *Corrosion Science*, *130*, pp.1-11.

Kovalenko, O.N., Kundo, N.N. and Kalinkin, P.N., 2001. Kinetics and mechanism of low-temperature oxidation of H2S with oxygen in the gas phase. *Reaction Kinetics and Catalysis Letters*, *72*(1), pp.139-145.

Mayrhofer, C., Niessner, R. and Baumann, T., 2014. Hydrochemistry and hydrogen sulfide generating processes in the Malm aquifer, Bavarian Molasse Basin, Germany. *Hydrogeology journal*, *22*(1), pp.151-162.

McFarland, Mark L.; Provin, T. L. (2014) Hydrogen Sulfide in Drinking Water Treatment Causes and Alternatives. Texas A&M University.

Milsch, H., Giese, R., Poser, M., Kranz, S., Feldbusch, E. and Regenspurg, S., 2013. FluMo—a mobile fluid–chemical monitoring unit for geothermal plants. *Environmental earth sciences*, *70*(8), pp.3459-3463.

Müller, D.R., Friedland, G. and Regenspurg, S., 2017. An improved sequential extraction method to determine element mobility in pyrite-bearing siliciclastic rocks. International journal of environmental analytical chemistry, 97(2), pp.168-188.

Nasution, A., Takashima, I., Muraoka, H., Takahashi, H., Matsuda, K., Akasako, H., Futagoishi, M., Kusnadi, D. and Nanlohi, F., 2000, May. The geology and geochemistry of Mataloko-Nage-Bobo geothermal areas, central Flores, Indonesia. In *Proceedings of World Geothermal Congress 2000, Beppu and Morioka, Japan* (pp. 2165-2170).

Puigdomenech, I., 2004. Hydra/Medusa chemical equilibrium database and plotting software. KTH Royal Institute of Technology.

Ramasamy, S., Singh, S., Taniere, P., Langman, M.J.S. and Eggo, M.C., 2006. Sulfide-detoxifying enzymes in the human colon are decreased in cancer and upregulated in differentiation. *American Journal of Physiology-Gastrointestinal and Liver Physiology*, *291*(2), pp.G288-G296.

Regenspurg, S., Brand, A. and Peiffer, S., 2004. Formation and stability of schwertmannite in acidic mining lakes. Geochimica et Cosmochimica Acta, 68(6), pp.1185-1197.

Reiffenstein, R.J., Hulbert, W.C. and Roth, S.H., 1992. Toxicology of hydrogen sulfide. *Annual review of pharmacology and toxicology*, *32*(1), pp.109-134.

Vairavamurthy, A. and Mopper, K., 1987. Geochemical formation of organosulphur compounds (thiols) by addition of H2S to sedimentary organic matter. *Nature*, *329* (6140), p.623.

Wiberg, N., Wiberg, E. and Holleman, A.F., 1995. Lehrbuch der Anorganischen Chemie, 101. Auflage. May, P.M., Batka, D., Hefter, G., Königsberger, E. and Rowland, D., 2018. Goodbye to S 2− in aqueous solution. Chemical communications, 54(16), pp.1980-1983.

Zötl, J.G., 1997. The spa Deutsch-Altenburg and the hydrogeology of the Vienna basin (Austria). *Environmental Geology*, *29*(3-4), pp.176-187.